High contrast transparent ramsey fringes using microwave pulses interaction with atomic coherent state in warm rubidium vapor

Yisheng Ma (马易升), Jianliao Deng (邓见辽), Zhengfeng Hu (胡正峰), Huijuan He (何慧娟), and Yuzhu Wang (王育竹)*

Key Laboratory for Quantum Optics, Center for Cold Atom Physics, Shanghai Institute of Optics and Fine Mechanics, Chinese Academy of Sciences, Shanghai 201800, China

**Corresponding author: yzwang@mail.shcnc.ac.cn*

Received May 25, 2012; accepted October 10, 2012; posted online January 30, 2013

High contrast transparent Ramsey fringes are observed using double microwave pulses interaction with the prepared atomic coherent state in a warm ^{87}Rb vapor with mixture buffer gases in a closed cell. The Ramsey fringes are generated by the pulsed technique, a strong coupling light pulse and a weak signal light pulse are applied to prepare the atomic coherent state, followed by the application of double microwave pulses to interact with the atomic coherent state. Afterwards, the light pulses are applied again with weaker intensity and detecting the signal transmission is delected. The central line of the transparent Ramsey fringes has narrow linewidth of 125 Hz and high contrast of 21%. The light shift is dramatically reduced since the interrogating process is not involved the light field, and the cavity pulling effect is negligible due to the low Q requirement, which is promising for building small, compact, and stable atomic clocks.

OCIS codes: 270.1670, 190.4180.
doi: 10.3788/COL201311.032701.

Small, compact, and stable atomic clock is wildly used in many application fields, such as navigation, telecommunication, and high-resolution spectroscopy nowadays. The applications demand local oscillators with high frequency stability in the short and the medium terms[1]. In order to improve the frequency stability, the pulsed method with many new physical concepts has been developed, such as the pulsed coherent population trapping technique[2,3], the pulsed optically pumped frequency standard[4], the Raman-Ramsey fringes in a double lambda system[5], and the formation of Ramsey fringes based on pulsed coherent light storage[6]. Through the time separation technique, the pulsed regime dramatically reduced or eliminated various physical effects, such as light shift, power shift and so on. Meanwhile, quantum interference effects induced by interacting atomic coherent states may lead to sharp, high-contrast resonances[7]. The resonances associated with the double-dark states can be made absorptive or transparent; moreover, their optical properties, such as width and position, can be manipulated by adjusting the coherent interaction[8−10].

Combining the advantages of the two above-mentioned techniques, we demonstrate the observation of the high contrast transparent Ramsey fringes in warm rubidium (Rb) vapor with mixture buffer gases in a closed cell. This obserration has promising applications in further improving the frequency stability of atomic clocks. The relevant energy levels and light and microwave fields are shown in Fig. 1. The technique can be understood qualitatively as follows. First, a strong coupling light pulse and a weak probe light pulse are applied to prepare the atomic coherent state in the Λ-type configuration and turned off smoothly, the population and atomic coherent state are preserved. Then Ramsey microwave pulses are applied to drive a magnetic-dipole transition between the fourth level and ground state. There is no light field involved during this stage. The atomic coherent state is modified and the population is excited to the ground state. Due to the change of the initial atomic state which contains the Ramsey microwave interaction information, when the coupling and signal light pulses are applied again with weaker intensity, the detected transient signal pulse has a gain part compared with that of the first preparation stage, which results in Ramsey fringes transparent.

A simple physical picture about the system can be described as follows. The coupling field (Rabi frequency Ω_c) and the signal field (Rabi frequency Ω_s) are represented by right and left circularly polarized light (σ^+ and σ^-), respectively, as derived from a single linear polarized light. These light fields couple pairs of Zeeman sublevels

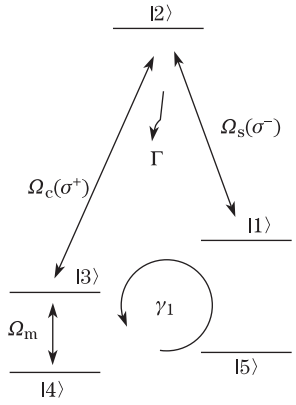

Fig. 1. Configuration of ^{87}Rb atomic states resonantly coupled to a coupling field (Ω_c), a signal field (Ω_s), and a microwave field (Ω_m). $|2\rangle=|^2 P_{1/2}, F=2, m_F=1\rangle$, $|1\rangle=|^2 S_{1/2}, F=2, m_F=2\rangle$, $|3\rangle=|^2 S_{1/2}, F=2, m_F=0\rangle$, $|4\rangle=|^2 S_{1/2}, F=1, m_F=0\rangle$.

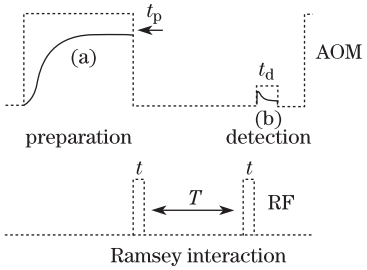

Fig. 2. Time sequence. t_p: preparing time; t: Rabi time; T: Ramsey time; t_d: detecting time. Transient signal evolution in the (a) preparation and (b) detection stages.

of ground state $(5^2S_{1/2})$ ^{87}Rb atoms with magnetic quantum numbers differing by two, via the excited $5^2P_{1/2}$,$F = 2$ state. As the ground-state sublevels have the same energies, the Hanle-EIT and related coherent effects can be observed around the zero magnetic field[11]. In this case, an additional microwave field couples the fourth state $|\ 5^2S_{1/2}, F = 1, m_F = 0\rangle$ to $|\ 5^2S_{1/2}, F = 2, m_F = 0\rangle$. In this experiment, the coupling field is much stronger than the signal field ($\Omega_c \gg \Omega_s$), most of the relevant atoms were pumped in the states $|\ 5^2S_{1/2}, F = 2, m_F = 2\rangle$ and $|\ 5^2S_1/2, F = 1, m_F = 0\rangle$. Thus, we can focus on the realistic system shown as $|\ 1\rangle$, $|\ 2\rangle$,$|\ 3\rangle$, and $|4\rangle$, respectively.

The evolution of the system can be analyzed by using ensemble-averaged density matrix formalism:

$$\dot{\rho} = \frac{1}{\mathrm{i}\hbar}[H, \rho] + \frac{\partial \rho}{\partial t}, \tag{1}$$

where ρ is the matrix density and H is the interacting Hamiltonian. Under the rotating wave approximation, the Hamiltonian is

$$H = -\hbar \begin{pmatrix} \Delta_c - \Delta_s & \Omega_s & 0 & 0 \\ \Omega_s & \Delta_c & \Omega_c & 0 \\ 0 & \Omega_c & 0 & \Omega_m \\ 0 & 0 & \Omega_m & -\Delta \end{pmatrix}, \tag{2}$$

where $\Delta_c = \omega_c - \omega_{23}$, $\Delta_s = \omega_s - \omega_{21}$, $\Delta = \omega_m - \omega_{34}$ are the detunings of coupling, signal and microwave fields, respectively. $\frac{\partial \rho}{\partial t}$ describes the relaxation of ρ and for simplification its elements are given as

$$\frac{\partial \rho_{22}}{\partial t} = -(\Gamma_1 + \Gamma_3 + \Gamma_4)\rho_{22}, \tag{3}$$

$$\frac{\partial \rho_{ii}}{\partial t} = \Gamma_i \rho_{22} + \gamma_1 \sum_{j \neq i} (\rho_{jj} - \rho_{ii}), (i, j = 1, 3, 4), \tag{4}$$

$$\frac{\partial \rho_{ij}}{\partial t} = -\Gamma_{ij}\rho_{ij}, (i, j = 1, 2, 3, 4), \tag{5}$$

with

$$\Gamma_{21} = \Gamma_{23} = \Gamma_{24} = \Gamma, \Gamma_{31} = \Gamma_{41} = \Gamma_{34} = \gamma_0, \tag{6}$$

where Γ_1, Γ_3, and Γ_4 are the spontaneous decay rates from $|2\rangle$ to $|1\rangle$, $|3\rangle$, and $|4\rangle$, respectively; γ_1 and γ_0 represent the population transfer and the hyperfine coherence ralaxation rates between the ground states, respectively; the interaction with buffer gases is included in the definition of the decay rates. The propagation of the signal field can be described by the Maxwell equation in the slowly varying amplitude approximation:

$$\frac{\partial \Omega_s}{\partial z} = -\eta Im(\rho_{21}), \tag{7}$$

where $\eta = \nu_1 N \wp_{21}^2 / 2\epsilon_0 c\hbar$ is the coupling constant.

The whole process can be separated into three stages, the preparation, interaction, and detection stages. The atomic coherent state preparation stage contains the optical pumping process as well. The coupling and signal lights are resonant turned on, $\Omega_s, \Omega_c \neq 0, \Omega_m = 0$, and $\Delta_c = \Delta_s = 0$. We can obtain

$$\begin{aligned} \dot{\rho_{11}} &= \Gamma_1 \rho_{22} + \Omega_s Im(\rho_{12}) + \gamma_1(\rho_{33} + \rho_{44} - 2\rho_{22}), \\ \dot{\rho_{21}} &= -\gamma \rho_{21} - \mathrm{i}\Omega_s(\rho_{22} - \rho_{11}) + \mathrm{i}\Omega_c \rho_{31}, \\ \dot{\rho_{31}} &= -\gamma_0 \rho_{31} + \mathrm{i}\Omega_c \rho_{21}. \end{aligned} \tag{8}$$

The experimental observed transient process is shown in Fig. 2(a). In the steady state with the case of $\Omega_s << \Omega_c$, $\rho_{22} \simeq 0, \rho_{33} \simeq 0$, and most of the atoms stay in the $|1\rangle$ and $|4\rangle$ states. The ρ_{31} and ρ_{21} can be derived as

$$\begin{aligned} \rho_{31}^0 &= -\frac{\Omega_s \Omega_c \rho_{11}^0}{\gamma\gamma_0 + \Omega_c^2}, \\ \rho_{21}^0 &= -\frac{0\Omega_s \gamma_0 \rho_{11}^0}{\gamma\gamma_0 + \Omega_c^2}, \end{aligned} \tag{9}$$

and when $\Omega_c^2 >> \gamma\gamma_0$,

$$\rho_{11}^0 = 1/2, \quad \rho_{21}^0 = 0, \quad \rho_{31}^0 = -\frac{\Omega_s}{2\Omega_c}. \tag{10}$$

Since the lights come from the same source, ρ_{31}^0 is constant, and the prepared state and population are quite immune to the light noise.

In the microwave interaction stage, we turn off the lights smoothly and apply two microwave pulses. Each microwave pulse lasts for time t, and the time interval during two microwave pulse is T. During this stage, $\Omega_s = \Omega_c = 0$, and the equations of density matrix are[1]

$$\begin{aligned} \dot{\rho_{33}} &= \Omega_m Im(\rho_{34}) + \gamma_1(\rho_{11} + \rho_{44} - 2\rho_{33}), \\ \dot{\rho_{31}} &= \mathrm{i}\Omega_m \rho_{41} - \gamma_0 \rho_{31}, \\ \dot{\rho_{41}} &= \mathrm{i}\Omega_m \rho_{31} + i\Delta_c \rho_{41} - \gamma_0 \rho_{41}. \end{aligned} \tag{11}$$

After the first microwave pulse,

$$\begin{pmatrix} \rho_{31}(t) \\ \rho_{41}(t) \end{pmatrix} = M(\Omega_m, \Delta, t) \begin{pmatrix} \rho_{31}^0 \\ \rho_{41}^0 \end{pmatrix}. \tag{12}$$

Here

$$M(\Omega_m, \Delta, t) = \mathrm{e}^{(\mathrm{i}\frac{\Delta}{2} - \gamma_0)t} \begin{pmatrix} \cos\xi t - \mathrm{i}\frac{\Delta}{2\xi}\sin\xi t & -\mathrm{i}\frac{\Omega_m}{\xi}\sin\xi t \\ -\mathrm{i}\frac{\Omega_m}{\xi}\sin\xi t & \cos\xi t + \mathrm{i}\frac{\Delta}{2\xi}\sin\xi t \end{pmatrix}, \tag{13}$$

with $\xi = \sqrt{(\Delta/2)^2 + \Omega_m^2}$. During the interrogation, the coherence decays freely, as shown by

$$M(0, \Delta, T) = \mathrm{e}^{-\gamma_3 T} \begin{pmatrix} 1 & 0 \\ 0 & \mathrm{e}^{\mathrm{i}\Delta T} \end{pmatrix}. \tag{14}$$

After the second microwave pulse, the coherence becomes

$$\begin{pmatrix}\rho_{31}(t)\\ \rho_{41}(t)\end{pmatrix}= M(\Omega_{\rm m},\Delta,t)M(0,\Delta,T)M(\Omega_{\rm m},\Delta,t)\begin{pmatrix}\rho^0_{31}\\ \rho^0_{41}\end{pmatrix}. \tag{15}$$

There is only coherence between $|\,1\rangle$ and $|\,3\rangle$ after the atomic coherent state is prepared. Meanwhile if the coherence of $\rho^0_{41}=0$, we can get

$$\begin{aligned}\rho_{31}(T+2t) = {\rm e}^{{\rm i}\Delta t-\gamma_0(T+2t)}[(\cos\xi t-{\rm i}\tfrac{\Delta}{2\xi}\sin\xi t)^2\\ -{\rm e}^{{\rm i}\Delta T}(\tfrac{\Omega_m}{\xi}\sin\xi t)^2]\rho^0_{31}.\end{aligned} \tag{16}$$

In the vicinity of $\Delta=0$ and $\Omega_{\rm m}t=\pi/2$, we can get a simplified formula:

$$\rho_{31}(T+2t)=\frac{-\Omega_{\rm s}}{2\Omega_{\rm c}}e^{-\gamma_0(T+2t)}\sin^2\Omega_{\rm m}t{\rm e}^{{\rm i}\Delta(T+t)}. \tag{17}$$

The population can be derived in a similar way and the expression can be written as

$$\begin{aligned}\rho_{33}(T+2t)=\frac{1}{2}\Big[\frac{2}{3}-\frac{1}{6}{\rm e}^{-3\gamma_1(T+2t)}\Big]\\ \cdot[1+\cos\Delta(T+t)]\sin^2\Omega_{\rm m}t.\end{aligned} \tag{18}$$

The coherence between the $|\,1\rangle$ and $|\,3\rangle$ states and the population in $|\,3\rangle$ state are shown in the Ramsey pattern (Figs. 3(a) and (b)).

In the signal detection stage, we turn on the light pluses again but with weaker intensity. During this stage, the initial condition has been modified, the transient evolution shows that a gain part pluss the normal absorption section compared with that of the first preparation stage. Many works related to these processes have been conducted[12−14]. We detect the intensity of the signal light and integrate it with time, and obtain transparent Ramsey fringes finally.

In order to observe the good experimental results, we make a lot of efforts to prepare the lab environment and experimental equipments. The experimental setup is shown in Fig. 4. The cell is made of the quartz and has a diameter $D=25$ mm and a length $L=30$ mm; it contains the warm pure ^{87}Rb vapor with mixture buffer gases Ar (15.5 Torr) and N_2 (9.5 Torr). The operating temperature is set to 63 °C. At this temperature, the atomic density is

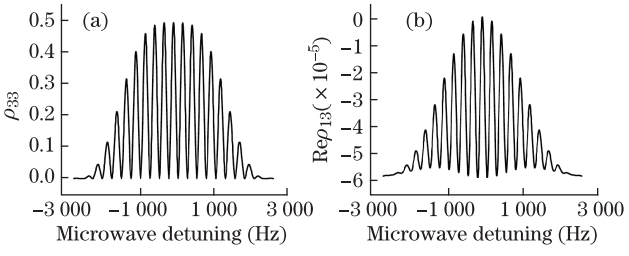

Fig. 3. Numerical simulation Ramsey fringes after two microwave pulses interact the atomic coherent state. (a) Population in the $|3\rangle$ state; (b) real part of the coherence between the $|3\rangle$ and $|1\rangle$ states. The parameters are $\Gamma=3\times10^9$ s^{-1}, γ_1=360, γ_0=300 s^{-1}, $\Omega_{\rm c}=2.8\times10^7$ s^{-1}, $\Omega_{\rm s}=1\times10^6$ s^{-1}, $\Omega_{\rm m}=2\times10^5$ s^{-1}.

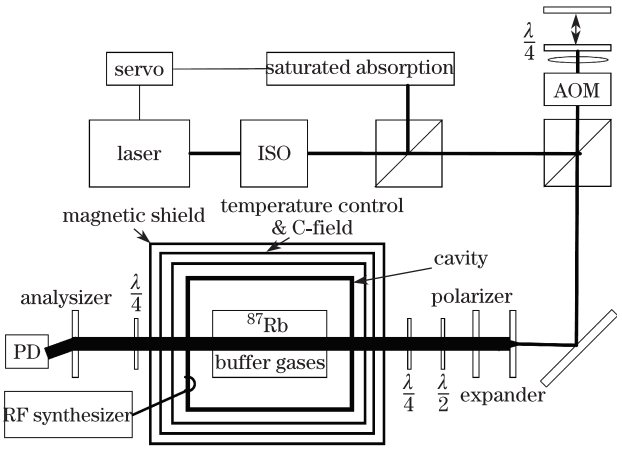

Fig. 4. Experimental setup.

$n=4\times10^{11}/{\rm cm}^3$, the buffer gas induced hyperfine frequency shift and optical shift are $\Delta'_{34}\simeq4$ kHz and $\Delta'_{23}=\Delta'_{21}=-170$ MHz, and the excited state decay rate is $\gamma=1.8\times10^9$ s^{-1}. The cell is placed inside a TE_{011} microwave cavity. The loaded quality factor is $Q_{\rm L}=410$; and the resonance frequency is tuned to about 6.834 GHz corresponding to magnetic-dipole transition of $|\,5^2S_{1/2},F=1,M_{\rm F}=0\rangle$ to $|\,5^2S_{1/2},F=2,M_{\rm F}=0\rangle$. Two-layer temperature controls are placed between the three-layer μ-metal shields, a precise cylindrical coil surrounds the microwave cavity. The temperature standard deviation $\sigma_{\rm T}$ of the cavity is $\sigma_{\rm T}<10$ mK for measuring time $\tau<20\,000$ s, the remnant magnetic field is less than 20 μG, the applied quantization field is 32 mG. The light frequency is stabilized by employing the saturated absorption spectroscopy technique. An acousto-optical modulator (AOM) which is set in the double-pass configuration shifts the light frequency of –170 MHz, and is also used as an intensity controller and switcher of the lights. We slightly rotate the polarization of the input light with a $\lambda/2$ and two $\lambda/4$ plates to generate a weak left circular polarized signal light (σ^-) and a strong right circular polarized coupling light (σ^+). The input light is collimated and expanded into a diameter of 8 mm and then passes through the sample cell. The signal and coupling lights are separated by a high-quality polarizer and analyzer with an extinction ratio of 1×10^{-5}, and detected using individual photo detectors.

In the first stage, we turn on and set the coupling light to 8 mW, and the signal light to 20 μW, the pulse duration $t_{\rm p}=3$ ms which is enough to prepare the atomic coherent state, and turn off the lights smoothly over about 3 μs. In the second stage, we set the microwave output power to –1 dBm, corresponding to $\Omega_{\rm m}\simeq4$ kHz measured by the way of Rabi oscillations, and the pulse duration $t=400$ μs, the free time T=3.6 ms. In the last stage, we turn on the two light pulses again with weaker intensity. The coupling light is 80 μW and the signal light is 200 nW with the duration of 0.6 ms. The transient evolution in this stage is different from that in the first stage since the initial condition has changed. the readout signal contains the information caused by the Ramsey microwave pulses interaction with the atomic coherent state. We leave about 2-ms blank time to let the system recover the natural state. Based on the central microwave

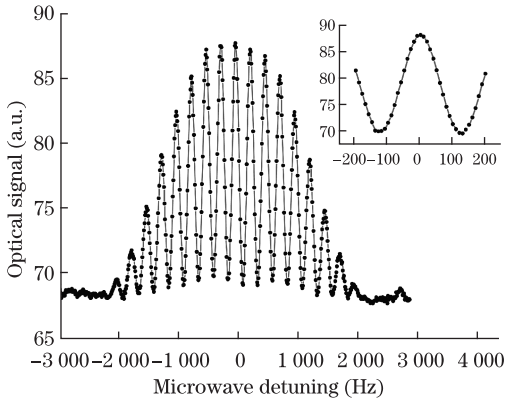

Fig. 5. Ramsey fringes by a single scanning process. The width is 125 Hz and the contrast is about 21%.

frequency of 6.834687032 GHz, we take 10 Hz per step to scan the microwave frequency from 6.834684 to 6.834690 kHz. The transparent Ramsey fringes are obtained by a single scanning process and have not involved any mathematics fitting and average (Fig. 5). The width is 125 Hz and the contrast reaches around 21%. The signal-to-noise ratio (SNR) of the central fringe is more than 140 times in the 1-kHz bandwidth. The main characteristic of the Ramsey fringe is the line-width. The line-width of the central zone of the Ramsey pattern are both about 125±4 Hz for the experimental and theoretical results, and they agree well with the well-known expression $\Delta\nu = 1/2T$.

The first advantage of this technique is the dramatics reduction of the light shift because the process which generates the main information of Ramsey fringes has not involved any light fields. The residual light shift is contributed from the preparation stage and detection stage. However, we can increase the coupling light intensity and decrease the signal light intensity in the first stage, which makes the prepared coherent and population immune to the light noise; it can also decrease the light intensity in the detection stage which makes the amplitude-to-frequency (AM-FM) and frequency-to-frequency (FM-FM) effects be very small. The light shift we obtained is smaller by a factor of 10^3 compared with the usual optically pumped Rb frequency standard from our measurement[1]. The second advantage of this technique is dramatic reduction of the cavity feedback as we only need a low Q microwave cavity, e.g. Q=300. We have found that the contrast of the central Ramsey fringe turns higher when the applied signal light intensity is weaker. Further research related to optimize the method will be required.

In conclusion, high contrast transparent Ramsey fringes are observed using double microwave pulses interaction with the prepared atomic coherent state in a warm ^{87}Rb vapor with mixture buffer gases in a closed cell. Combining the pulsed method and the atomic coherent state perturbation technique, it is dramatically reduced of the light shift, and is free of the cavity pulling effect. It is very promising to build compact atomic clocks with high frequency stability.

We thank Jinda Lin for useful help. This work was supported by the Major State Basic Research Development Program of China under Grant No. 2005CB724507.

References

1. J. Vanier and C. Audoin, *The Quantum Physics of Atomic Frequency Standards* (Adam-Hilger, Bristol, 1989).
2. J. Vanier, Appl. Phys. B: Lasers and Optics **81,** 421 (2005).
3. G. S. Pati, F. K. Fatemi, and M. S. Shahriar, Opt. Express **19,** 22388 (2011).
4. A. Godone, S Micalizio, and F Levi, Phys. Rev. A **70,** 023409 (2004).
5. T. Zanon, S. Guerandel, E. De Clercq, and D. Holleville, Phys. Rev. Lett, **94,** 193002 (2005).
6. B. Yan, Y. Ma, and Y. Wang, Phys. Rev. A **79,** 063820 (2009).
7. C. Deutsch, F. Ramirez-Martinez, C. Lacroûte, F. Reinhard, T. Schneider, J. N. Fuchs, F. Piechon, F. Laloë, J. Reichel, and P. Rosenbusch, Phys. Rev. Lett **105,** 020401 (2010).
8. M. D. Lukin, S. F Yelin, M. Fleischhauer, and M. O. Scully, Phys. Rev. A **60,** 3225 (1999).
9. Y.-C. Chen, Y.-A. Liao, H.-Y. Chiu, J.-J. Su, and I. A. Yu, Phys. Rev. A **64,** 053806 (2001).
10. Y. Niu, S. Gong, R. Li, Z. Xu, and X. Liang, Opt. Lett. **30,** 3371 (2005).
11. W. Hanle, Z. Phys. **30,** 93 (1924).
12. Y. Li and M. Xiao, Opt. Lett. **20,** 1489 (1995).
13. H. X. Chen, A. V. Durrant, J. P. Marangos, and J. A. Vaccaro, Phys. Rev. A **58,** 1545 (1998).
14. S. J, Park, H. Cho, T. Y. Kwon, and H. S. Lee, Phys. Rev. A **58,** 023806 (2004).